Intermolecular Interaction of Stiff-Chain Polymers in Solution

Takahiro Sato,* Yuji Jinbo, and Akio Teramoto

Department of Macromolecular Science, Osaka University, Toyonaka, Osaka 560, Japan

Received July 1, 1996; Revised Manuscript Received November 13, 1996[⊗]

ABSTRACT: The effects of polymer chain ends and polydispersity in the molecular weight were incorporated into the perturbation theory based on the scaled particle theory for wormlike spherocylinder solutions, which was previously used to analyze thermodynamic properties of stiff or semiflexible polymer solutions in terms of intermolecular interactions. The modified theory was applied to three stiff or semiflexible polymer solutions, poly(*n*-hexyl isocyanate)−*n*-hexane, schizophyllan−water, and poly(γ-benzyl L-glutamate)−dimethylformamide, to estimate the intermolecular interaction parameters (the hard-core diameter d and the strength of the soft attraction). The values of d estimated for all the polymers are reasonably compared with the diameter calculated from the partial specific volume. The soft attractive interaction and the polymer-chain-end effect were significant for schizophyllan, but unimportant for poly(*n*-hexyl isocyanate) and poly(γ-benzyl L-glutamate).

1. Introduction

The intermolecular interaction of neutral polymers in solution consists of the hard-core repulsion and soft attraction. In good solvents, the former is predominant, while in poor solvents, both interactions are competitive. The two interactions can be characterized by the diameter (d) of the hard-core and a parameter (δ) related to the binary cluster integral with respect to the soft attractive potential (cf. eq 2 in the following).[1] The second virial coefficient (A_2), which is usually used as a measure of the solvent quality, is proportional to $d + \delta$.

In a previous study,[1] we proposed a procedure for estimating d and δ separately by the analysis of the osmotic compressibility $\partial c/\partial \Pi$ at finite concentrations and A_2 using a perturbation theory and applied the procedure to a semiflexible polymer, poly(*n*-hexyl isocyanate) (PHIC), in dichloromethane (DCM). The value of d estimated was 1.07 nm, which was favorably compared with the diameter calculated from the partial specific volume of the polymer, and the absolute value of δ was about one-third of d, which indicates that DCM is a medium solvent for PHIC.

Since the analysis was concerned with considerably high molecular weight PHIC samples with sufficiently narrow molecular weight distributions, we did not consider the effects of polymer chain ends and also of polydispersity in the previous data analysis of $\partial c/\partial \Pi$ and A_2. However, those effects are not always negligible. Recently Yamakawa et al.[2−4] pointed out that the effect of polymer chain ends is important to A_2 of flexible polymers even at relatively high molecular weights. In addition to this, thermodynamic properties of stiff-chain polymer solutions were often studied by using polymer samples with appreciably broad molecular weight distributions. Therefore, it may be important to take into account these two effects for theoretical analyses. In the present study, we have corrected for these effects the previous procedure to estimate d and δ. Theoretical considerations of these effects are described in section 2.

We use this new procedure for analyzing data on three stiff-chain polymer systems, schizophyllan in water, poly(γ-benzyl L-glutamate) (PBLG) in dimethylformamide (DMF), and PHIC in *n*-hexane. Thermodynamic properties required to apply the procedure have already been measured for schizophyllan[5,6] and PBLG[7,8] solutions. On the other hand, the osmotic compressibility for PHIC in *n*-hexane was measured by sedimentation equilibrium in the present study. Section 3 describes the experimental details, and section 4 analyzes data of thermodynamic properties for PHIC in *n*-hexane as well as for schizophyllan in water and PBLG in DMF to estimate intermolecular interaction parameters.

2. Theoretical Section

A. Polymer-Chain-End Effect. In the previous study,[1] thermodynamic quantities for a wormlike spherocylinder (WSC) solution were formulated by a perturbation theory. The quantities for the reference hard WSC solution were derived by the scaled particle theory,[9,10] while the thermodynamic perturbation due to a weak soft potential between two WSC was incorporated up to the second virial term. The scaled particle theory for the reference solution takes into account the end effect of the hard WSC on the thermodynamic quantities. However, the perturbation term does not include the WSC end effect of the soft potential. Here, we consider this effect by calculating the binary cluster integral ($\langle\beta_w\rangle$) with respect to the soft interaction potential (w) of the WSC.[11]

The soft potential (w) between two WSC can be calculated by

$$w = \int_{-L/2}^{L/2} \mathrm{d}s_1' \int_{-L/2}^{L/2} \mathrm{d}s_2'\, G(x) \qquad (1)$$

where L is the contour length of the WSC, and $G(x)$ is the local van der Waals free energy per unit contour length in solution, which is a function of the distance x between the interacting contour elements $\mathrm{d}s'_1$ and $\mathrm{d}s'_2$; s_i' (i = 1, 2) is the contour distance from the middle of contour of the chain i, which ranges from $-L/2$ to $L/2$. McLachlan[12,13] expressed $G(x)$ in terms of dielectric polarizabilities of the interacting elements and the dielectric permeability of the solvent. Since $G(x)$ is defined in solution, w should be regarded as the potential of mean force. If the polymer chain ends (or the hemispheres of the WSC) possess different interaction properties from those of the middle portion, $G(x)$ also depends on the contour points s_1' and s_2' at $|s_1'|, |s_2'| \gtrsim L_c/2 - \Delta$. Here, L_c is the contour length of the cylinder part of the WSC which is equal to $L - d$ with the WSC hard-core diameter d, and Δ is a maximum distance where $G(x)$ takes a nonzero value.

[⊗] Abstract published in *Advance ACS Abstracts,* January 15, 1997.

S0024-9297(96)00938-2 CCC: $14.00

Let us specify the two closest approaching points of the two WSC contours by the contour distances s_1 and s_2 from the middle of each contour. When s_i (i =1 and 2) are not close to $\pm L/2$, i.e., $|s_i| < L_c/2 - \Delta$, we can approximate w to that between two infinitely long WSC, denoted by w_∞. On the other hand, when s_i (i =1 and/or 2) are close to $\pm L/2$, we cannot use this approximation for w. We refer to the former and latter configurations of two WSC as the crossed and noncrossed configurations, respectively.

The binary cluster integral ($\langle\beta_w\rangle$) is given as the sum of the contributions of the crossed and noncrossed configurations. These contributions are presented in Appendices of the previous[1] and present papers, respectively. The total cluster integral is written in the form

$$-\frac{1}{2}\langle\beta_w\rangle = \frac{\pi}{4}(L')^2\left[\delta + \delta'\left(\frac{d}{L'}\right) + \delta''\left(\frac{d}{L'}\right)^2\right] \tag{2}$$

where $L' \equiv L - d/3$, and δ , δ', and δ'' are the soft interaction parameters defined by eqs A2 and A5 in the Appendix. While δ represents the strength of the soft interaction in the crossed configuration, δ' and δ'' characterize, respectively, the soft interactions between middle and end portions and between end portions of two WSC in the noncrossed configuration. $\langle ... \rangle$ represents the average with respect to the conformation and orientation of the two WSC.

The soft potential w of the mean force in the noncrossed configuration can be either attractive or repulsive, depending on affinity among polymer middle and end portions and the solvent.[14] Thus δ' and δ'' can be either positive or negative. On the other hand, the soft potential w_∞ between neutral polymer chains of the same kind in the crossed configuration should be attractive,[14] so that the sign of δ must be negative.

We use the shift factor M_L, the molar mass per unit contour length of the cylinder part of the WSC, to relate L to the molecular weight M by

$$L = \frac{M}{M_L} + \frac{d}{3} \tag{3}$$

Here we have assumed that the end hemispheres and middle cylinder of the WSC have the same density. Using this shift factor, we rewrite eq 2

$$-\frac{1}{2}\langle\beta_w\rangle = \frac{\pi M^2}{4M_L^2}\left[\delta + \delta'\frac{dM_L}{M} + \delta''\left(\frac{dM_L}{M}\right)^2\right] \tag{4}$$

With this result, the second virial coefficient A_2 is given by

$$A_2 = \frac{\pi d N_A}{4M_L^2}\left[1 + \frac{\delta}{d} + \left(\frac{8}{3} + \frac{\delta'}{d}\right)\frac{dM_L}{M} + \left(\frac{4}{9} + \frac{\delta''}{d}\right)\left(\frac{dM_L}{M}\right)^2\right] \tag{5}$$

where N_A is the Avogadro constant and the hard-core terms of A_2 were obtained from the scaled particle theory.[10] The correction terms in eq 5 associated with the polymer chain ends have the same form as Yamakawa's result[2] for A_2, which was derived using a bead model.

B. Polydispersity Effect. Thermodynamic quantities for solutions of polydisperse hard WSC were calculated by the scaled particle theory.[9,10] After perturbation terms are included, the results for the osmotic pressure (Π) and the chemical potential (μ_s) of the WSC species s in an isotropic state are given by

$$\frac{\Pi}{k_B T} = \frac{c'}{1 - \bar{v}c'} + \frac{Bc'^2}{2(1 - \bar{v}c')^2} + \frac{2Cc'^3}{3(1 - \bar{v}c')^3} - \frac{1}{2}\sum_{s,t=1}^{r} x_s x_t \langle\beta_{w,st}\rangle c'^2 \tag{6}$$

$$\frac{\mu_s}{k_B T} = \frac{\mu_s^\circ}{k_B T} + \ln\left(\frac{x_s c'}{1 - \bar{v}c'}\right) + \frac{(B_s + v_s)c'}{(1 - \bar{v}c')} + \frac{\left(C_s + \frac{1}{2}Bv_s\right)c'^2}{(1 - \bar{v}c')^2} + \frac{2Cv_s c'^3}{3(1 - \bar{v}c')^3} - \sum_{t=1}^{r} x_t \langle\beta_{w,st}\rangle c' \tag{7}$$

where c' is the total number concentration, x_s the mole fraction of species s, $\bar{v}$ the number-average volume of WSC, $\langle\beta_{w,st}\rangle$ the averaged binary cluster integral for species s and t, and μ_s° and v_s the standard chemical potential and the molecular volume of species s, respectively. The coefficients B, C, B_s, and C_s are defined in ref 9, in terms of the contour length L_s and hard-core diameter d of the WSC species s. We assume that all WSC species have the same diameter.

It is convenient to rewrite the above equations in terms of experimentally measurable quantities, the number-average molecular weight (M_n) and the total polymer mass concentration (c). Using the shift factor M_L, c is related to the total polymer volume fraction (ϕ) by

$$\phi = \frac{\pi d^2 N_A}{4M_L} c \tag{8}$$

Calculating the coefficients B, C, B_s, and C_s according to eqs 10 of ref 9, we obtain

$$\frac{\Pi}{cRT} = \frac{1}{M_n} + \phi\left[\frac{F_1(\phi)}{dM_L} + \frac{F_2(\phi)}{M_n} + \frac{F_3}{2M_n^2}\right] \tag{9}$$

$$\frac{\mu_s}{k_B T} = \frac{\mu_s^\circ}{k_B T} + \ln\left(\frac{w_s}{v_s}\right) + \ln\left(\frac{\phi}{1 - \phi}\right) + M_s\phi\left[\frac{F_4(\phi)}{dM_L} + \frac{F_2(\phi)}{M_n} + \frac{F_5(\phi)}{M_s} + \frac{F_3}{M_n M_s}\right] \tag{10}$$

where w_s is the weight fraction of species s in the total polymer. The coefficients F_i ($i = 1 - 5$) are defined by

$$F_1(\phi) = \frac{3 + \phi}{3(1 - \phi)^3} + \frac{\delta}{d} \tag{11a}$$

$$F_2(\phi) = \frac{8 - 7\phi + 3\phi^2}{3(1 - \phi)^3} + \frac{\delta'}{d} \tag{11b}$$

$$F_3 = 2M_L\delta'' \tag{11c}$$

$$F_4(\phi) = \frac{6 - 3\phi + \phi^2}{3(1 - \phi)^3} + 2\frac{\delta}{d} \tag{11d}$$

$$F_5(\phi) = \frac{5 - 3\phi}{3(1 - \phi)^2} + \frac{\delta'}{d} \tag{11e}$$

To obtain eqs 11, we have extended the result of eq 4

for the case of two WSC with different lengths, assuming δ, δ', and δ'' to be independent of the polymer species. In eq 11c, we have omitted terms due to the hard-core potential, which are negligibly small.

Thermodynamic properties of polymer solutions were often studied by sedimentation equilibrium experiment. In 1970, Scholte[15] proposed a method of analyzing sedimentation equilibrium data for polydisperse polymer solutions on the basis of the Flory−Huggins theory. Here, we modify his method by replacing the Flory−Huggins theory by the perturbation theory.

The sedimentation equilibrium condition is given by[16,17]

$$\frac{1}{RT}M_s\left(\frac{\partial\rho}{\partial c}\right)\omega^2 r = \frac{1}{k_B T}\frac{\mathrm{d}\mu_s}{\mathrm{d}r} \tag{12}$$

where R is the gas constant, $\partial\rho/\partial c$ the partial specific density increment, ω the angular velocity, and r the distance from the centrifugal center to some position of the solution column under consideration. Here the density (ρ) has been assumed to depend on c but not on the polymer composition w_s. Since the scaled particle theory treats a system at constant T and solvent (or diffusible component) chemical potential (μ_D), one should use $\partial\rho/\partial c$ at constant T and μ_D. For single solvent systems, $\partial\rho/\partial c$ at constant T and μ_D can be approximated to that at constant T and pressure.

According to Scholte's treatment, we can obtain the following equation from eqs 10 and 12

$$Z(r) \equiv \frac{c(r)(\partial\rho/\partial c)\omega^2 r}{RT\,\mathrm{d}c(r)/\mathrm{d}r} = \frac{1}{M_w(r)} + \phi\left\{\frac{F_6(\phi)}{dM_L} + \frac{F_2(\phi)}{M_w(r)} + \frac{F_7(\phi)}{M_n(r)} + \frac{F_3}{M_n(r)M_w(r)} - Y\frac{(F_2(\phi) + F_3/M_w(r))[1 + \phi(F_2(\phi) + F_3/M_n(r))]}{1 + \phi F_3 Y}\right\} \tag{13}$$

with

$$F_6(\phi) = 2\left[\frac{1+\phi}{(1-\phi)^4} + \frac{\delta}{d}\right] \tag{11f}$$

and

$$F_7(\phi) = \frac{2}{3}\left[\frac{4+\phi+\phi^2}{(1-\phi)^4}\right] + \frac{\delta'}{d} \tag{11g}$$

$$Y = \frac{1}{M_n(r)} - \frac{1}{M_w(r)}$$

The left-hand side of eq 13 can be determined by a sedimentation equilibrium experiment. In a usual low-speed experiment of sedimentation equilibrium for concentrated solutions, $c(r)$, $M_n(r)$, and $M_w(r)$ at the middle portion of the solution column can be approximated to c, M_n, and M_w of the original solution, respectively. For a polymer sample with a narrow distribution, the term proportional to Y in eq 13 is negligible, and thus the right-hand side of eq 13 can be approximated by $(RT)^{-1}\partial\Pi/\partial c$ for a monodisperse polymer solution with the molecular weight M equal to $M_w(r)$, which is given from eq 9 by

$$\frac{1}{RT}\frac{\partial\Pi}{\partial c} = \frac{1}{M} + \phi\left[\frac{F_6(\phi)}{dM_L} + \frac{F_2(\phi)+F_7(\phi)}{M} + \frac{F_3}{M^2}\right] \tag{14}$$

Table 1. Molecular Characteristics of the PHIC Samples Used

sample	$M_w/10^4$	$A_2/10^{-4}$ cm^3 g^{-2} mol	M_w/M_n[a]
No-15	1.80[b]	9.5[b]	1.04
No-34	7.25[b]	10.8[b]	1.03
	7.94[c]	10.1[c]	
NRX-VII-d	11.7[c]	9.2[c]	1.07

[a] Determined by GPC. [b] Determined by sedimentation equilibrium. [c] Determined by light scattering.[19]

Equation 6 gives us the osmotic second virial coefficient A_2^{OS} in the form

$$A_2^{OS} = \frac{\pi d N_A}{4M_L^2}\left[1 + \frac{\delta}{d} + \left(\frac{8}{3} + \frac{\delta'}{d}\right)\frac{dM_L}{M_n} + \left(\frac{4}{9} + \frac{\delta''}{d}\right)\left(\frac{dM_L}{M_n}\right)^2\right] \tag{15}$$

On the other hand, using eq 7, thermodynamic theories[17] for light scattering and sedimentation equilibrium yield the second virial coefficients for light scattering (A_2^{LS}) and for sedimentation equilibrium (A_2^{SE}) as

$$A_2^{LS} = A_2^{SE} = \frac{\pi d N_A}{4M_L^2}\left[1 + \frac{\delta}{d} + \left(\frac{8}{3} + \frac{\delta'}{d}\right)\frac{dM_L}{M_w} + \left(\frac{4}{9} + \frac{\delta''}{d}\right)\left(\frac{dM_L}{M_w}\right)^2\right] \tag{16}$$

where M_w is the weight-average molecular weight. The equality of A_2^{SE} with A_2^{LS} holds in a low-speed experiment.[17]

C. Method of Determining the Interaction Parameters. Equation 15 or 16 can be rewritten as

$$(A_2^X - A_{2,\infty}^X)M_x = I + S/M_x \tag{17}$$

where

$$A_{2,\infty}^X = \frac{\pi N_A}{4M_L^2}(d+\delta) \qquad I = \frac{\pi d N_A}{4M_L}\left(\frac{8}{3}d + \delta'\right)$$

$$S = \frac{\pi d^2 N_A}{4}\left(\frac{4}{9}d + \delta''\right) \tag{18}$$

[$(X, x) = $ (OS, n), (LS, w), or (SE, w)]. The second virial coefficient $A_{2,\infty}^X$ without including the polymer-chain-end effect can be equated to A_2^X at sufficiently high molecular weight. On the other hand, the quantities I and S may be estimated by the intercept and slope, respectively, of the plot of $(A_2^X - A_{2,\infty}^X)M_x$ vs $1/M_x$. This procedure of estimating I and S was originally applied to flexible polymer solutions by Einaga et al.,[3] although $A_{2,\infty}^X$ must be calculated theoretically for this case.

If some value is chosen for d, the values of δ, δ', and δ'' can be calculated, respectively, from $A_{2,\infty}^X$, I, and S estimated by the above procedure using eqs 18, and furthermore Π or $Z(r)$ using eqs 9 or 13 with these interaction parameters. The value of d may be determined by fitting the calculated Π or $Z(r)$ to experimental results up to high concentrations. This procedure will be applied to some stiff-chain polymer solutions in section 4.

3. Experimental Section

Three fractionated samples of PHIC were chosen from our stock for sedimentation equilibrium experiment. The polydispersity index M_w/M_n, determined by GPC, was less than 1.1 for all the samples (cf. Table 1).

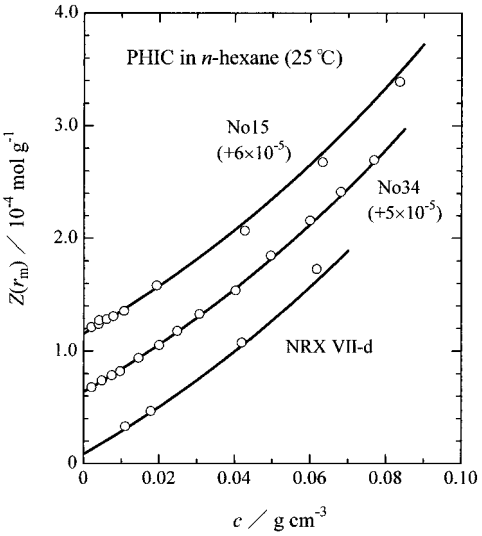

Figure 1. Sedimentation equilibrium data for *n*-hexane solutions of three PHIC samples at 25 °C: (○) experimental data of $Z(r_m)$ (cf. eq 13), (−) theoretical values calculated by eq 13 with $d = 1.10$ nm. The data points and theoretical curves for samples No-15 and No-34 are shifted upward by the amount indicated in the parentheses.

A sedimentation equilibrium experiment for *n*-hexane solutions of PHIC was done at 25 °C by using a Beckman−Spinco model E ultracentrifuge. The concentration distribution in PHIC solutions under a centrifugal field was determined using the Rayleigh interference optics at $c < 5 \times 10^{-2}$ g/cm^3 and using the Schlieren optics at higher concentrations. The rotor speed was chosen at a value between 6800 and 15 000 rpm for each PHIC sample, and the length of the solution column was adjusted to ca. 1.5 mm.

From the sedimentation equilibrium data for dilute solutions, the weight-average molecular weight (M_w) and the second virial coefficient (A_2^{SE}) were determined for samples No-15 and No-34 by the conventional method.[5] The polydispersity effect on A_2^{SE} was negligible under the above-mentioned experimental conditions. The results are listed in Table 1.

For concentrated solutions, the quantity $Z(r_m)$ defined by eq 13 at $r = r_m$ was calculated from sedimentation equilibrium data as a function of the polymer concentration c and M_w. For most sedimentation equilibrium experiments performed, $c(r)$ at the middle portion r_m of the solution column agreed with c of the original solution within 1%.

To calculate $Z(r_m)$, $\partial\rho/\partial c$ and $\partial n/\partial c$ (the specific refractive index increment) were determined for *n*-hexane solutions of PHIC at 25 °C over the concentration range examined by sedimentation equilibrium. The results were 0.368 for $\partial\rho/\partial c$ and 0.126 cm^3/g for $\partial n/\partial c$ (at 546 nm), irrespective of c up to 0.11 g/cm^3. These results are in good agreements with those determined by Murakami et al.[18] in a low-c region.

4. Results and Discussion

A. Poly(*n*-hexyl isocyanate) in *n*-Hexane. Figure 1 shows the plots of $Z(r_m)$ against c for three PHIC samples in *n*-hexane at 25 °C. The intercepts of the plots for samples No-15 and No-34 give the values of $M_w(r_m)$ (cf. eq 13) which agree with M_w obtained from the conventional data analysis.[16−18] The data points for each sample follow a curve convex downward. This curvature indicates the breakdown of the second virial approximation for the PHIC solutions at high concentrations, because $Z(r_m)$ should be identified with $(RT)^{-1}\partial\Pi/\partial c$ in a good approximation (cf. eqs 13 and 14) for the PHIC samples with narrow molecular weight distributions (see Table 1).

Figure 2 shows A_2^{LS} and A_2^{SE} data for PHIC in *n*-hexane at 25 °C obtained by Murakami et al.[18]

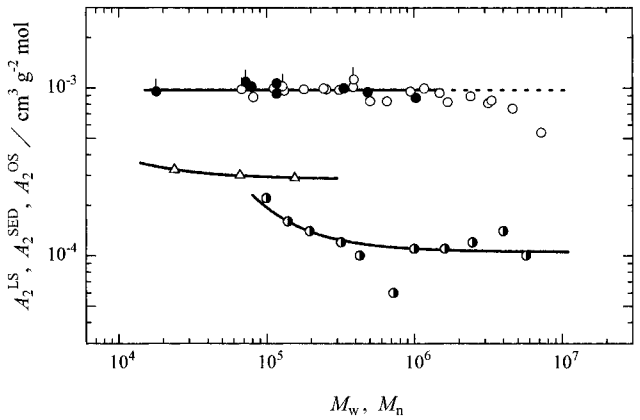

Figure 2. Molecular weight dependence of the second virial coefficient for PHIC in 25 °C *n*-hexane (○, ●[18]), schizophyllan in 25 °C water (◑[5]), and PBLG in 30 °C DMF (△[7]). The experimental methods are identified by circles with and without pips for A_2^{SE} and A_2^{LS}, respectively, and triangles for A_2^{OS}; the theoretical values calculated by eq 16 (or eq 18) with the parameters listed in Table 2 are indicated by the solid curves.

(unfilled circles), by Jinbo et al.[19] (filled circles without pips), and in the present study (filled circles with pips; cf. Table 1). It can be seen that A_2^{LS} and A_2^{SE} are almost independent of M_w at $M_w \lesssim 2 \times 10^6$ but A_2^{LS} decreases at higher M_w. The constant second virial coefficient indicates that the polymer end effect is not important for PHIC in *n*-hexane, while the decrease of A_2^{LS} at higher M_w may be ascribed to the effect of multiple contacts between two long PHIC chains, which is not considered in eq 16.[20] In the following data analysis using the perturbation theory explained in section 2, we neglect the A_2^{LS} data at $M_w > 2 \times 10^6$.

We obtain 9.7×10^{-4} cm^{3}g^{-2} mol by averaging A_2^{LS} and A_2^{SE} at M_w between 3×10^5 and 2×10^6 and take this value as $A_{2,\infty}^X$, the second virial coefficient without including the polymer-chain-end effect (X = LS or SE). This average value gives the relation $d + \delta = 1.09$ nm from eq 16; here we used 730 nm^{-1} for M_L of PHIC in *n*-hexane estimated recently by Norisuye et al.[21]

Using this $A_{2,\infty}^X$ and the ten low molecular weight data of A_2^X, we plot $(A_2^X - A_{2,\infty}^X)M_w$ against $1/M_w$ in Figure 3 (filled and unfilled circles). Although the plotted points are slightly scattered, they appear to follow the solid line in the figure with the zero intercept and slope. From eqs 18 with $I = S = 0$, we can estimate the ratios of δ'/d and δ''/d to be $-8/3$ and $-4/9$, respectively. However, the factors dM_L/M_w and its square in eq 16 are so small at $M_w \gtrsim 1 \times 10^4$ (cf. Table 2 for the value of d) that the estimates of δ'/d and δ''/d are not decisive.

Using the above three relations among d, δ, δ', and δ'', we searched for a value of d which leads to the best fit of eq 13 to experimental results of $Z(r_m)$ shown in Figure 1. In this search, $M_w(r_m)$ and $M_n(r_m)$ were equated to M_w and M_n of the original PHIC samples (cf. Table 1), and the volume fraction ϕ was calculated by eq 8 with c and d chosen. The solid curves in Figure 1 represent the theoretical values for $Z(r_m)$ with the optimum d value of 1.10 nm, which are seen to reproduce the data for the three PHIC samples. The values of the interaction parameters d, δ, δ', and δ'' determined are summarized in Table 2. As mentioned above, the values of δ' and δ'' contain some uncertainties, but they may not affect the determination of d and δ, because of small contributions of the polymer end effect to $Z(r_m)$ at $M_w \gtrsim 1 \times 10^4$.

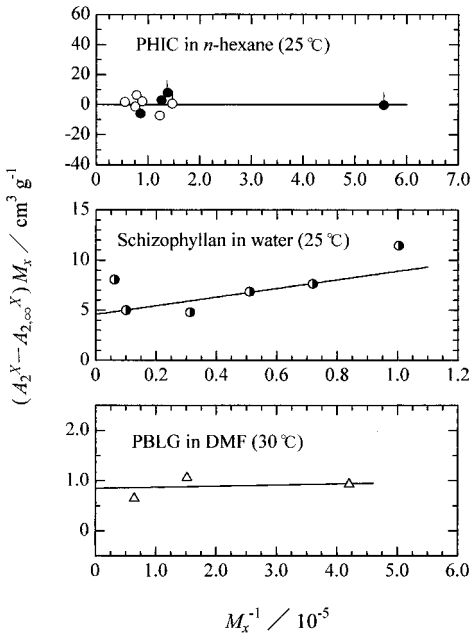

Figure 3. Plots of $(A_2^X - A_{2,\infty}^X)M_x$ vs $1/M_x$ for PHIC in *n*-hexane, schizophyllan in water, and PBLG in DMF. The symbols are the same as those in Figure 2.

Table 2. Interaction Parameters of Stiff-Chain Polymers in Solution

polymer	solvent	d/nm	δ/nm	δ'/nm	δ''/nm	d_v/nm[a]
PHIC	*n*-hexane	1.10	−0.01	−2.9	−0.5	1.21
	DCM	1.07[b]	−0.36[b]			1.25
schizophyllan	water	1.75	−0.72	7.3	300	1.68
PBLG	DMF	1.42	−0.13	−1.9	2	1.56

[a] Calculated by $d_v = (4v_{sp}M_L/\pi N_A)^{1/2}$ from the partial specific volume (v_{sp}). [b] Estimated in ref 1.

For each sample, the values of $Z(r_m)$ calculated by eq 13 closely agreed with $(RT)^{-1}\partial\Pi/\partial c$ calculated by eq 14 with $M = M_w$ and the values of d, δ, δ', and δ'' listed in Table 2. Therefore, the polydispersity effect is not important for our fractionated PHIC samples. In a previous study,[1] we analyzed data of $Z(r_m)$ and A_2 for PHIC with $M_w > 1 \times 10^5$ in dichloromethane using eq 14, without considering the effects of polydispersity and polymer chain ends. The unimportance of both the effects for fractionated PHIC samples justifies the previous analysis.

B. Schizophyllan in Water. Yanaki et al.[5] measured A_2^{SE} for a rigid triple helical polysaccharide, schizophyllan, in water by sedimentation equilibrium. Figure 2 reproduces their results with half-filled circles. Although the data points are scattered, A_2^{SE} shows an upswing at $M_w \lesssim 3 \times 10^5$, while it appears to be constant at higher M_w. We ascribe this upswing to the polymer-chain-end effects embodied in eq 16.

Figure 3 shows the plot of $(A_2^{SE} - A_{2,\infty}^{SE})M_w$ vs $1/M_w$ for schizophyllan in water with half-filled circles. Here we have used the experimental data at $M_w < 2 \times 10^6$ (except for two small A_2^{SE} data) and the value $1.0_5 \times 10^{-4}$ cm^3 g^{-2} mol for $A_{2,\infty}^{SE}$. From this plot, we have estimated I and S to be 4.6 cm^3/g and $4._3 \times 10^5$ cm^3/mol, respectively (cf. the straight line indicated in the figure).[22] The solid curve in Figure 2 is drawn by using eq 17 with the values of $A_{2,\infty}^{SE}$, I, and S determined.

Van and Teramoto[6] presented $Z(r_m)$ data for aqueous solutions of schizophyllan up to the vicinity of the isotropic−cholesteric phase boundary concentration.[23] Their results are shown by circles in Figure 4. As in

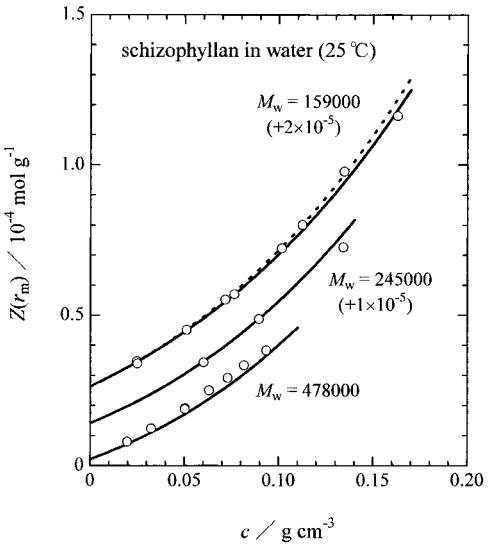

Figure 4. Concentration dependence of $Z(r_m)$ for aqueous solutions of schizophyllan at 25 °C: (○) experimental data obtained by Van and Teramoto,[6] (−) theoretical values calculated by eq 13, (...) theoretical values for the lowest molecular weight sample without considering the polydispersity effect (calculated with eq 14). The data points and theoretical curves except for the highest molecular weight sample are shifted upward by the amount indicated in the parentheses.

the case of *n*-hexane solutions of PHIC, a d value fitting eq 13 to those experimental results was sought by trial and error. In eq 13, δ, δ', and δ'' were calculated by eqs 18 with d chosen and $A_{2,\infty}^{SE}$, I, and S estimated above. In eq 13, the values of M_n [$=M_n(r_m)$] were estimated from M_z/M_w (=1.2) measured for the samples by assuming the Schultz−Zimm distribution (i.e., $M_n/M_w = 2 - M_z/M_w$), and the reference value[5] of 2150 nm^{-1} was used for M_L.

The solid curves in Figure 4, representing theoretical values for d = 1.75 nm, satisfactorily agree with the data points for all the three schizophyllan samples. The interaction parameters estimated for the schizophyllan−water system are listed in Table 2.

If the effect of polydispersity in the molecular weight is neglected, $Z(r_m)$ becomes identical with $(RT)^{-1}\partial\Pi/\partial c$ (cf. section 2B), and its theoretical values are slightly changed, as indicated by the dotted curve for the lowest molecular weight sample in Figure 4. Here we have used eq 14 with $M = M_w$ and the same interaction parameters. Therefore, the neglect of the polydispersity effect may provide some error in determining the interaction parameters. It is noted that the fitting shown by the solid curve in Figure 4 is better than the previous fitting[10,24] considering neither intermolecular soft interactions ($\delta = \delta' = \delta'' = 0$) nor the sample polydispersity.

C. Poly(γ-benzyl L-glutamate) in Dimethylformamide. Kubo and Ogino[7,8] measured the osmotic pressure (Π) and A_2^{OS} for DMF solutions of PBLG. Their results are shown with circles in Figure 5 and with triangles in Figure 2, respectively. Using these data, we estimated the interaction parameters of PBLG in DMF. First, the A_2^{OS} data was analyzed with eq 17. The values of $A_{2,\infty}^{OS}$, I, and S were determined to be 2.9×10^{-4} cm^3 g^{-2} mol, 0.85 cm^3/g, and 2×10^3 cm^3/mol, respectively (cf. Figure 3), and these values reproduce the A_2^{OS} data as shown by the solid curve in Figure 2.

The osmotic pressure data[25] were compared with eq 9. When d is chosen to be 1.42 nm, the theoretical

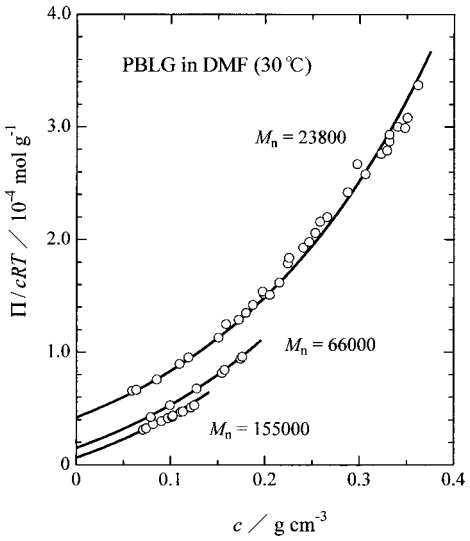

Figure 5. Concentration dependence of Π for DMF solutions of PBLG at 30 °C: (○) experimental data obtained by Kubo and Ogino,[7,8] (−) theoretical values calculated by eq 9.

curves shown in Figure 5 fit closely to the data points. Here we have used 1450 nm^{-1} for M_L.[26] The interaction parameters are listed in Table 2. However, the value of δ'' may not be decisive due to the scatter of the data points shown in Figure 3.

5. Concluding Remarks

The present study estimated the intermolecular interaction parameters (d, δ, δ', and δ'') for three stiff-chain polymer solutions, PHIC in *n*-hexane, schizophyllan in water, and PBLG in DMF. Table 2 summarizes the results along with the previous results[1] for PHIC in dichloromethane (DCM). (For the PHIC−DCM system, the effect of polymer-chain ends was not considered, because the previous analysis was made only for high molecular weight PHIC samples.) The values of the hard-core diameter (d) estimated for all the polymers are reasonably compared with the diameter (d_v) calculated from the partial specific volume (v_{sp}) listed in the seventh column of Table 2. So far, isotropic−liquid crystal phase boundary concentrations for various stiff-chain polymer solutions were often analyzed by using d_v.[10] The good agreement between d and d_v in Table 2 justifies the previous analyses.

While the values of d of PHIC in *n*-hexane and DCM are close each other, $|\delta|$ of PHIC in *n*-hexane is much smaller than that in DCM. This indicates that the soft attractive interaction is less important for PHIC in *n*-hexane than in DCM. From the value of $|\delta|$, it turns out that the soft attractive interaction is of minor importance for PBLG in DMF but appreciable for schizophyllan in water.

The triple helix of schizophyllan was reported to be unstable in water at very low molecular weights.[27] This suggests that the helix is unwound at its ends, and thus the unwound ends of the helix may have interaction properties considerably different from those of the middle portion. The large values of $|\delta'|$ and $|\delta''|$ for schizophyllan may reflect this difference.

Acknowledgment. The authors wish to thank Professor T. Norisuye in our Department, for valuable comments and discussion, and also one of the reviewers, for important comments. This work was partially supported by a Grant-in-Aid for Scientific Research from the Ministry of Education, Science, and Culture of Japan.

Appendix

The binary cluster integral ($\langle\beta_w\rangle$) with respect to the soft potential (w) of mean force of the WSC can be calculated by[1]

$$\langle\beta_w\rangle = \int_{-l}^{l} ds_1 \int_{-l}^{l} ds_2\, 2\delta + 2\int_{-l}^{l} ds_1 \int_{l}^{l'} ds_2\, 2\delta_{nc} + 2\int_{-l}^{l} ds_1 \int_{-l'}^{-l} ds_2\, 2\delta_{nc} + \int_{l}^{l'} ds_1 \int_{l}^{l'} ds_2\, 2\delta_{nc} + 2\int_{l}^{l'} ds_1 \int_{-l'}^{-l} ds_2\, 2\delta_{nc} + \int_{-l'}^{-l} ds_1 \int_{-l'}^{-l} ds_2\, 2\delta_{nc} \quad \text{(A1)}$$

Here $l \equiv L_c/2 - \Delta$, $l' \equiv L/2 + \Delta$

$$\delta \equiv -\frac{4}{\pi}\int_d^\infty dr' \left\langle \left| \mathbf{a}(s_1) \times \mathbf{a}(s_2) \right| \left[\exp\left(-\frac{w_\infty}{k_B T} \right) - 1 \right] \right\rangle \quad \text{(A2)}$$

and

$$\delta_{nc} \equiv -\frac{4}{\pi}\int_{d'}^\infty dr' \left\langle \exp\left(-\frac{w_{nc}}{k_B T} \right) - 1 \right\rangle \quad \text{(A3)}$$

where r' is the distance between the closest contour points s_1 and s_2, $\mathbf{a}(s_i)$ is the unit tangent vector to the contour point s_i, d' is the shortest distance between s_1 and s_2 when the WSC hard cores do not overlap in the noncrossed configuration, w_∞ and w_{nc} are w in the crossed and noncrossed configurations, respectively, and $\langle ... \rangle$ represents the average with respect to the conformation and orientation of the two WSC.

Writing the kth term I_k in the right-hand side of eq A1 as

$$I_k = \begin{cases} (L_c - \Delta)\left(\Delta + \frac{1}{4}d\right)\delta_k & (k = 2,3) \\ \left(\Delta + \frac{1}{4}d\right)^2 \delta_k & (k = 4,5,6) \end{cases} \quad \text{(A4)}$$

we obtain eq 2 in the text, where the interaction parameters δ' and δ'' are defined by

$$\begin{cases} \delta' \equiv \frac{4}{\pi}\left(\Delta' + \frac{1}{4}\right)(\delta_2 + \delta_3) - 4\left(\Delta' + \frac{1}{2}\right)\delta \\ \delta'' \equiv 4\left(\Delta' + \frac{1}{2}\right)^2 \delta - \frac{8}{\pi}\left(\Delta' + \frac{1}{2}\right)\left(\Delta' + \frac{1}{4}\right)(\delta_2 + \delta_3) + \frac{4}{\pi}\left(\Delta' + \frac{1}{4}\right)^2 (\delta_4 + \delta_5 + \delta_6) \end{cases} \quad \text{(A5)}$$

with $\Delta' \equiv \Delta/d$. In the liquid crystalline state, the parameter δ depends on the degree of orientation, while δ_k ($k = 2 - 6$) are approximately independent of the degree of orientation.

References and Notes

(1) Jinbo, Y.; Sato, T.; Teramoto, A. *Macromolecules* **1994**, *27*, 6080.
(2) Yamakawa, H. *Macromolecules* **1992**, *25*, 1912.
(3) Einaga, Y.; Abe, F.; Yamakawa, H. *Macromolecules* **1993**, *26*, 6243.
(4) Abe, F.; Einaga, Y.; Yamakawa, H. *Macromolecules* **1994**, *27*, 3262.
(5) Yanaki, T.; Norisuye, T.; Fujita, H. *Macromolecules* **1980**, *13*, 1462.
(6) Van, K.; Teramoto, A. *Polym. J.* **1985**, *17*, 409.
(7) Kubo, K.; Ogino, K. *Mol. Cryst. Liq. Cryst.* **1979**, *53*, 207.
(8) Kubo, K. *Mol. Cryst. Liq. Cryst.* **1981**, *74*, 71.
(9) Sato, T.; Shoda, T.; Teramoto, A. *Macromolecules* **1994**, *27*, 164.

(10) Sato, T.; Teramoto, A. *Adv. Polym. Sci.* **1996**, *126*, 85.
(11) A similar calculation was previously made, when the polymer-end effect on the electrostatic interaction between stiff polyelectrolytes was taken into account.[28]
(12) McLachlan, A. D. *Proc. R. Soc. London* **1963**, *A271*, 387.
(13) McLachlan, A. D. *Proc. R. Soc. London* **1963**, *A274*, 80.
(14) Israelachvili, J. N. *Q. Rev. Biophys.* **1974**, *6*, 341.
(15) Scholte, T. G. *J. Polym. Sci., Part A-2* **1970**, *8*, 84.
(16) Fujita, H. *Foundation of Ultracentrifugal Analysis*; Wiley-Interscience: New York, 1975.
(17) Kurata, M. *Thermodynamics of Polymer Solutions*; Harwood Academic Publishers: Chur, 1982.
(18) Murakami, H.; Norisuye, T.; Fujita, H. *Macromolecules* **1980**, *13*, 345.
(19) Jinbo, Y.; Sato, T.; Teramoto, A. *Polym. J.*, submitted.
(20) Sato, T.; Jinbo, Y.; Teramoto, A. *Polym. J.* **1995**, *27*, 384.
(21) Norisuye, T.; Tsuboi, A.; Teramoto, A. *Polym. J.* **1996**, *28*, 357.
(22) The lowest molecular weight schizophyllan sample used by Yanaki et al. might contain some single chain component dissociated from the triple helix, because the molecular weight in water is less than 3 times of that in dimethyl sulfoxide.[5,27] Therefore, we have neglected this data point when drawing the straight line in Figure 3.
(23) Van and Teramoto also conducted a light-scattering experiment for concentrated schizophyllan solutions. We have not analyzed their light-scattering data in this study, because no relevant theory including the effects of polymer ends and polydispersity is available to analyze the data.
(24) Sato, T.; Teramoto, A. *Mol. Cryst. Liq. Cryst.* **1990**, *178*, 143.
(25) Ogino and Kubo also measured Π for anisotropic solutions of PBLG. However, there is no relevant expression of Π for anisotropic solutions of polydisperse polymers, and thus we have not analyzed their data for the anisotropic solutions.
(26) Itou, S.; Nishioka, N.; Norisuye, T.; Teramoto, A. *Macromolecules* **1981**, *14*, 904.
(27) Yanaki, T.; Itou, W.; Tabata, K.; Kojima, T.; Norisuye, T.; Takano, N.; Fujita, H. *Biophys. Chem.* **1983**, *17*, 337.
(28) Sato, T.; Teramoto, A. *Physica* **1991**, *A176*, 72.

MA9609386